

## Design of Tensegrity Structures with Static and Dynamic Modal Requirements

Raman Goyal<sup>1</sup>, Edwin A. Peraza Hernandez<sup>2</sup>, Manoranjan Majji<sup>3</sup> and Robert E. Skelton<sup>4</sup>

<sup>1</sup>Graduate Student, Department of Aerospace Engineering, Texas A&M University, College Station, TX 77843, USA; email: ramaniitrgoyal92@tamu.edu

<sup>2</sup>Assistant Professor, Department of Mechanical and Aerospace Engineering, University of California, Irvine, Irvine, CA 92697, USA; email: eperazah@uci.edu

<sup>3</sup>Assistant Professor, Department of Aerospace Engineering, Texas A&M University, College Station, TX 77843, USA; email: mmajji@tamu.edu

<sup>4</sup>TEES Eminent Professor, Department of Aerospace Engineering, Texas A&M University, College Station, TX 77843, USA; email: bobskelton@tamu.edu

### ABSTRACT

Over the last years, it has been theoretically demonstrated that tensegrity provides minimal mass solutions to load-bearing structures under static forces. Loading types including compressive forces, cantilever forces, uniformly distributed forces in simply-supported structures, and torsional forces have been considered. This paper extends the design of tensegrity structures beyond the support of static loads. Formulations and computational approaches for the design of minimal mass tensegrities that satisfy modal requirements such as targeted critical buckling forces and natural frequencies are presented. Implementation examples for both types of requirements considering beam-like geometries are provided. The results indicate that tensegrities provide minimal mass solutions to structures with static and dynamic modal requirements, as compared to continuum counterparts, extending the applicability of tensegrity systems in aerospace and civil engineering.

### INTRODUCTION

Tensegrity structures are stable truss-like constructions having pre-stressable capabilities and members with prescribed loading direction (tensile *strings/cables* and compressive *bars/struts*). These structures have obtained significant attention in Earth and space applications as different tensegrity topologies have been demonstrated to support static forces with *minimal mass* (Skelton and de Oliveira 2010; Nagase and Skelton 2014; De Tommasi et al. 2017; Ma et al. 2019; Carpentieri et al. 2017). Minimal mass in the context of tensegrities refers to that of a structure with the thinnest possible members which can support an external force distribution without local or global failure. Different types of load distributions such as compressive forces, cantilever forces, uniformly distributed forces in simply-supported structures, and torsional forces have all been considered. Other minimal mass applications of tensegrity structures under external forces include energy absorption (Rimoli 2016; Goyal

et al. 2019; Peraza Hernandez et al. 2018) and energy dissipation (Zhao and Peraza Hernandez 2019; Oppenheim and Williams 2001).

Unlike general truss structures, tensegrities possess two characteristics that are exploited in their minimal mass design (Skelton and de Oliveira 2010) and controllability (Chan et al. 2004; van de Wijdeven and de Jager 2005): *i*) their members have prescribed loading direction (*i.e.*, they are either compressive bars or tensile strings); and *ii*) they are pre-stressable (the load distribution within their members can be altered even in the absence of externally applied forces). In this paper, we make use of these characteristics to design minimal mass tensegrity structures with modal requirements (*e.g.*, target critical buckling forces and natural frequencies). The formulation for the quantification of these properties is derived in a general setting applicable to tensegrities of arbitrary geometry, topology, and mechanical boundary conditions. Beam-like structures are considered to provide example results of this new kind of tensegrity structural design. Tensegrities with engineered critical buckling forces and/or natural frequencies extend the applicability of these structures in the aerospace and civil engineering realms.

## LINEARIZED TENSEGRITY DYNAMICS

The non-linear dynamics of tensegrity systems are linearized in this section to obtain formulations for the modal properties of tensegrities (*e.g.*, critical buckling forces and natural frequencies). The non-linear dynamics are fully described by a compact second-order matrix differential equation that does not require the use of transcendental functions.

The number of nodes, strings, and bars in a tensegrity system are denoted by  $\nu$ ,  $\tau$ , and  $\beta$ , respectively. The matrix  $N = [n_1 \ n_2 \ \cdots \ n_\nu] \in \mathbb{R}^{3 \times \nu}$  contains the node position vectors  $n_i \in \mathbb{R}^3$ . The acceleration vectors of the nodes are contained in the matrix  $\ddot{N} = [\ddot{n}_1 \ \ddot{n}_2 \ \cdots \ \ddot{n}_\nu] \in \mathbb{R}^{3 \times \nu}$ . The external force matrix  $W = [w_1 \ w_2 \ \cdots \ w_\nu] \in \mathbb{R}^{3 \times \nu}$  contains the vectors of external force  $w_i \in \mathbb{R}^3$  applied to the nodes. The vectors along the length of the strings and bars are denoted  $s_j \in \mathbb{R}^3$  and  $b_k \in \mathbb{R}^3$ , respectively. The string connectivity matrix  $C_s \in \mathbb{R}^{\tau \times \nu}$  and bar connectivity matrix  $C_b \in \mathbb{R}^{\beta \times \nu}$  are incidence matrices that provide the information of the start and end nodes of each string and each bar, respectively. Using the connectivity information, the matrices containing the string and bar vectors are written as  $S = NC_s^\top = [s_1 \ s_2 \ \cdots \ s_\tau] \in \mathbb{R}^{3 \times \tau}$  and  $B = NC_b^\top = [b_1 \ b_2 \ \cdots \ b_\beta] \in \mathbb{R}^{3 \times \beta}$ , respectively. The compact matrix form for the full system dynamics is given as follows (Goyal and Skelton 2019):

$$\ddot{N}M + NK = W, \quad (1)$$

where the matrix  $K \in \mathbb{R}^{\nu \times \nu}$  is given by:

$$K = C_s^\top \hat{\gamma} C_s - C_b^\top \hat{\lambda} C_b, \quad (2)$$

and  $M \in \mathbb{R}^{\nu \times \nu}$  is analogous to a time-invariant mass matrix. The force density in the  $j^{\text{th}}$  string (magnitude of tensile force per unit length) is denoted by  $\gamma_j$  and the force density in the  $k^{\text{th}}$  bar (magnitude of compressive force per unit length) is denoted by  $\lambda_k$ . The diagonal matrices  $\hat{\gamma} \in \mathbb{R}^{\tau \times \tau}$  and  $\hat{\lambda} \in \mathbb{R}^{\beta \times \beta}$  are obtained by arranging  $\gamma_j$  and  $\lambda_k$  in their diagonal components, respectively.

The model for tensegrity non-linear dynamics in Eqs. (1) and (2) is linearized at an equilibrium configuration to obtain the following expression:

$$\mathbb{M}_L d\ddot{n} + \mathbb{K}_L dn = dw, \quad (3)$$

where  $dn = [dn_1^\top \ dn_2^\top \ \cdots \ dn_\nu^\top]^\top \in \mathbb{R}^{3\nu}$  is a vector containing small variations of the node positions vectors, and  $dw = [dw_1^\top \ dw_2^\top \ \cdots \ dw_\nu^\top]^\top \in \mathbb{R}^{3\nu}$  is a vector containing small variations of external forces at all the nodes. The time-invariant mass matrix  $\mathbb{M}_L \in \mathbb{R}^{3\nu \times 3\nu}$  is given as follows:

$$\mathbb{M}_L = \left( \frac{1}{12} C_b^\top \hat{m}_b C_b + C_{rb}^\top \hat{m}_b C_{rb} + \frac{1}{12} C_s^\top \hat{m}_s C_s + C_{rs}^\top \hat{m}_s C_{rs} \right) \otimes I_3, \quad (4)$$

where the matrices  $C_{rb} = \frac{1}{2}|C_b|$  and  $C_{rs} = \frac{1}{2}|C_s|$  ( $|\cdot|$  represents the element-wise absolute value of a matrix) are used to determine the center of mass of each bar and string, respectively. The diagonal matrices  $\hat{m}_s \in \mathbb{R}^{\tau \times \tau}$  and  $\hat{m}_b \in \mathbb{R}^{\beta \times \beta}$  are obtained by arranging the mass of each string and bar in their diagonal components, respectively, and  $I_3 \in \mathbb{R}^{3 \times 3}$  is the identity matrix and  $\otimes$  indicates the Kronecker product. The linearized global stiffness matrix  $\mathbb{K}_L \in \mathbb{R}^{3\nu \times 3\nu}$  is recently discussed in (Goyal et al. 2020):

$$\mathbb{K}_L = (C_s^\top \otimes I_3) \text{b.d.}(\cdots, K_{s_j}, \cdots)(C_s \otimes I_3) - (C_b^\top \otimes I_3) \text{b.d.}(\cdots, K_{b_k}, \cdots)(C_b \otimes I_3). \quad (5)$$

The contributions of the  $j^{\text{th}}$  string and the  $k^{\text{th}}$  bar to the global stiffness matrix  $\mathbb{K}_L$  are denoted by  $K_{s_j} \in \mathbb{R}^{3 \times 3}$  and  $K_{b_k} \in \mathbb{R}^{3 \times 3}$ , respectively:

$$K_{s_j} \triangleq \gamma_j I_3 + E_{s_j} A_{s_j} \frac{s_j s_j^\top}{l_{s_j}^3}, \quad K_{b_k} \triangleq \lambda_k I_3 - E_{b_k} A_{b_k} \frac{b_k b_k^\top}{l_{b_k}^3}, \quad (6)$$

where  $E_{s_j}$  and  $A_{s_j}$  are the Young's modulus and the cross-section area of the  $j^{\text{th}}$  string, respectively. Similarly,  $E_{b_k}$  and  $A_{b_k}$  respectively denote the Young's modulus and the cross-section area of the  $k^{\text{th}}$  bar.

## FORMULATION AND DESIGN APPROACH FOR TENSEGRITIES WITH TARGET CRITICAL BUCKLING FORCES

The string force density vector  $\gamma = [\gamma_1 \ \gamma_2 \ \cdots \ \gamma_\tau]^\top \in \mathbb{R}^\tau$  and the bar force density vector  $\lambda = [\lambda_1 \ \lambda_2 \ \cdots \ \lambda_\beta]^\top \in \mathbb{R}^\beta$  are written as the sum of force densities due to pre-stress  $(\gamma_p, \lambda_p)$  and force densities due the external forces  $(\gamma_w, \lambda_w)$  as:

$$\gamma = \gamma_p + \gamma_w, \quad \lambda = \lambda_p + \lambda_w, \quad (7)$$

where the force densities due to pre-stress (self-equilibrated under zero external force) are solved using the static equilibrium equation as (Goyal and Skelton 2019):

$$(C_b^\top \otimes I_3) \hat{B} \lambda_p = (C_s^\top \otimes I_3) \hat{S} \gamma_p, \quad \gamma_p \geq 0, \quad \lambda_p \geq 0, \quad (8)$$

where  $\hat{S} = \text{b.d.}(s_1, s_2, \dots, s_\tau) \in \mathbb{R}^{3\tau \times \tau}$  and  $\hat{B} = \text{b.d.}(b_1, b_2, \dots, b_\beta) \in \mathbb{R}^{3\beta \times \beta}$  are the body diagonal matrices formed by arranging the string vectors  $s_j$  and bar vectors  $b_k$  along their body diagonals, respectively. The force densities due to the external forces given by  $w = f\bar{w}$  are scaled by the scalar force parameter  $f$  as:

$$(C_b^\top \otimes I_3) \hat{B} \bar{\lambda}_w + \bar{w} = (C_s^\top \otimes I_3) \hat{S} \bar{\gamma}_w, \quad \bar{\gamma}_w \geq 0, \quad \bar{\lambda}_w \geq 0, \\ \text{with } \gamma_w = f\bar{\gamma}_w, \lambda_w = f\bar{\lambda}_w, \quad (9)$$

where  $\bar{w}$  is the non-dimensional external force vector used to represent the load distribution in the structure.

Using Eqs. (8) and (9), the linearized global stiffness matrix from Eq. (5) is reformulated as:

$$K_{s_j} = (\gamma_{p_j} + f\bar{\gamma}_{w_j})I_3 + E_{s_j} A_{s_j} \frac{s_j s_j^\top}{\|s_j\|^3}, \quad K_{b_k} = (\lambda_{p_k} + f\bar{\lambda}_{w_k})I_3 - E_{b_k} A_{b_k} \frac{b_k b_k^\top}{\|b_k\|^3}. \quad (10)$$

Global instability in a tensegrity structure arises if there exist non-trivial values of displacement in the structure ( $dn \neq 0$ ) under no changes in the values of the external forces ( $dw = 0$ ) (cf. Eq. (3)):

$$\mathbb{K}_L dn = 0. \quad (11)$$

Equation (11) has non-trivial solutions for  $dn$ , *if and only if*, the determinant of the symmetric global stiffness matrix  $\mathbb{K}_L$  is zero. Thus, the critical buckling force for any tensegrity structure is the value of force parameter  $f$  for which the global stiffness matrix  $\mathbb{K}_L$  is singular for given values of force density due to pre-stress and area of the members.

The minimum mass structure with targeted critical buckling force,  $f_{cr}$ , can be designed by minimizing the cross-section areas of the members  $(A_{s_j}, A_{b_k})$  and/or

pre-stress parameter ( $\bar{\gamma}$ ) such that the matrix  $\mathbb{K}_L$  reaches singularity for  $f = f_{cr}$ . The dimensionless pre-stress parameter is defined as  $\bar{\gamma} = \min[\gamma_p^\top \lambda_p^\top]$  such that Eq. (8) is satisfied. The lower bound on the cross-section area of all the members is obtained from two local failure criteria, yielding and buckling, as:

$$A_{s_j} \geq \frac{\gamma_j \|s_j\|}{\sigma_s}, \quad A_{b_k} \geq \max(A_{bY_k}, A_{bB_k}),$$

$$\text{where } A_{bY_k} = \frac{\lambda_k \|b_k\|}{\sigma_b}, \quad A_{bB_k} = 2 \|b_k\|^{\frac{3}{2}} \left( \frac{\lambda_k}{\pi E_b} \right)^{\frac{1}{2}}, \quad (12)$$

where  $\sigma_s$  and  $\sigma_b$  are the yield strengths of the strings and bars, respectively, and  $E_b$  is the Young's modulus of the bars.

## FORMULATION AND DESIGN APPROACH FOR TENSEGRITIES WITH TARGET NATURAL FREQUENCIES

The natural frequencies of a tensegrity structure are calculated from the linearized form of the non-linear dynamics model (Eq. (1)). The unforced solution of the linearized dynamics equation (Eq. (3)) provides the natural frequencies of the structure. Let us assume that the unforced solution of the linearized dynamic equation is of the form:

$$dn = \phi e^{\omega t}. \quad (13)$$

Substituting for  $dn$  from Eq. (13) into the linearized dynamics in Eq. (3) yields:

$$(\mathbb{M}_L \omega^2 + \mathbb{K}_L) \phi = 0, \quad (14)$$

where different values of  $\omega$  represent the natural frequencies of the system that are solved using Eq. (14) as the generalized eigenvalue problem. The generalized eigenvector  $\phi$  corresponding to each generalized eigenvalue represents the mode shape associated with the corresponding natural frequency. As no external forces are included in the calculation of natural frequencies of the system, the linearized global stiffness matrix from Eq. (5) contains only the contribution from the pre-stress as:

$$K_{s_j} = \gamma_{p_j} I_3 + E_{s_j} A_{s_j} \frac{s_j s_j^\top}{\|s_j\|^3}, \quad K_{b_k} = \lambda_{p_k} I_3 - E_{b_k} A_{b_k} \frac{b_k b_k^\top}{\|b_k\|^3}, \quad (15)$$

and the mass matrix  $\mathbb{M}_L$  is a function of only the cross-section area of all the members in the system. The minimum mass structure with targeted natural frequencies,  $\omega_{cr}$ , is designed by optimizing the cross-section areas of the members ( $A_{s_j}, A_{b_k}$ ) and pre-stress parameter ( $\bar{\gamma}$ ) such that the solution of the generalized

eigenvalue problem solved in Eq. (14) matches the targeted natural frequencies,  $\omega = \omega_{cr}$ . Equation (12) is also used to define the lower bound of the cross-section areas of the members to avoid local failure.

## RESULTS

This section presents results associated with the design of tensegrity structures with targeted modal requirements. Beam structures are considered as representative examples. The mass needed for the tensegrity structures to satisfy specified modal requirements is compared against that of continuum solid beams with the same modal properties. Material parameters representative of aluminum are assumed in all the examples (Young's moduli  $E_s = E_b = 60$  GPa, yield strengths  $\sigma_s = \sigma_b = 110$  MPa, and mass densities  $\rho_s = \rho_b = 2700$  kg/m<sup>3</sup>). All the calculations performed in the subsequent examples were implemented in MATLAB®. Optimization of the tensegrity structural parameters used to obtain the modal requirements while minimizing mass is performed using the function `fmincon` (MATLAB-fmincon 2020).

### Compressively loaded, simply-supported beam with target critical buckling forces

This example considers simply-supported beam structures, which are those that respectively have pin and roller boundary conditions at their ends. Continuum solid beams and three-dimensional tensegrity box structures are considered for critical buckling force comparisons and mass assessments.

**Critical buckling forces of a continuum solid beam.** The critical buckling forces of a continuum solid beam are obtained here using Euler theory of buckling (Johnston 1983). The beam has length  $l$  and is subjected to a compressive force of magnitude  $f$  applied at its end-points. The beam is composed of a linear elastic material with Young's modulus  $E_b$  and mass density  $\rho_b$ . The beam has a uniform rectangular cross-section with side lengths  $b$  and  $h$ . The critical buckling force of this beam is given as follows:

$$f_{cr} = \frac{i^2 \pi^2 E_b b h^3}{12 l^2}, \quad i = 1, 2, 3, \dots, \quad (16)$$

where  $i$  indicates the buckling mode. Furthermore, the deflection  $w$  in the buckled configuration is given as:

$$w = w_{max} \sin\left(\frac{i\pi x}{l}\right), \quad (17)$$

where  $w_{max}$  is the maximum deflection of the beam and  $0 \leq x \leq l$ .

**Critical buckling forces of a tensegrity beam.** Three-dimensional tensegrity box structures are used to approximate beams in this work. The parameters defining the tensegrity box structures are illustrated in Figure 1. Just as the continuum beams, the box structures have length  $l$  and rectangular cross-section of side lengths  $b$  and  $h$ . The complexity  $q$  of the box indicates the number of sections by which it is divided along its axial direction. The box supports a compressive force  $f$ , which is uniformly distributed among the four nodes at each end face of the box as indicated in Figure 1. The nodes at the two end faces of the box are constrained from moving on the  $y$ - and  $z$ -directions.

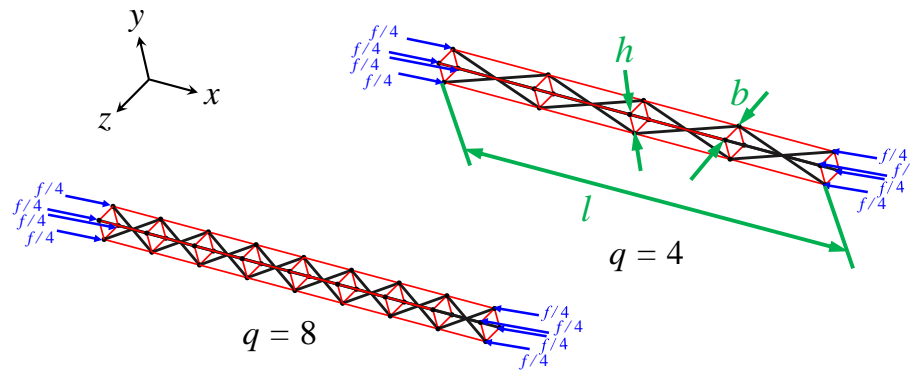


**Figure 1. Geometric parameters and applied loading for three-dimensional tensegrity box structures of complexities  $q = 4$  and  $q = 8$ .**

The three-dimensional tensegrity box structure is designed to match the first critical buckling force  $f_{cr}$  of a continuum solid beam. Figure 2 shows the first three buckling modes for a tensegrity box structure with  $h = b = 0.05$  m,  $l = 1$  m and  $q = 21$ , which is designed to match the first critical buckling force of a continuum beam  $f_{cr} = 308425$  N calculated from Eq. (16). Notice that the first three mode shapes of the tensegrity beam qualitatively match the continuum mode shapes described using Eq. (17).

The formulation given earlier is used to optimize the structure parameters to simultaneously minimize the mass of the tensegrity structure and to match the minimum critical buckling load of the continuum beam. Two different design approaches are used to perform this task: i) Adjusting the pre-stress in the structure, and ii) Adjusting the member cross-section areas. The *mass ratio* ( $\mu$ ) defined as the ratio of the mass of the approximated tensegrity beam  $m_T$  to the mass of the continuum beam  $m_B$  is given as follows:

$$\mu = \frac{m_T}{m_B}, \quad \text{where} \quad m_B = \rho_b b h l, \quad m_T = \rho_b \sum_{k=1}^{\beta} A_{b_k} l_{b_k} + \rho_s \sum_{j=1}^{\tau} A_{s_j} l_{s_j}. \quad (18)$$

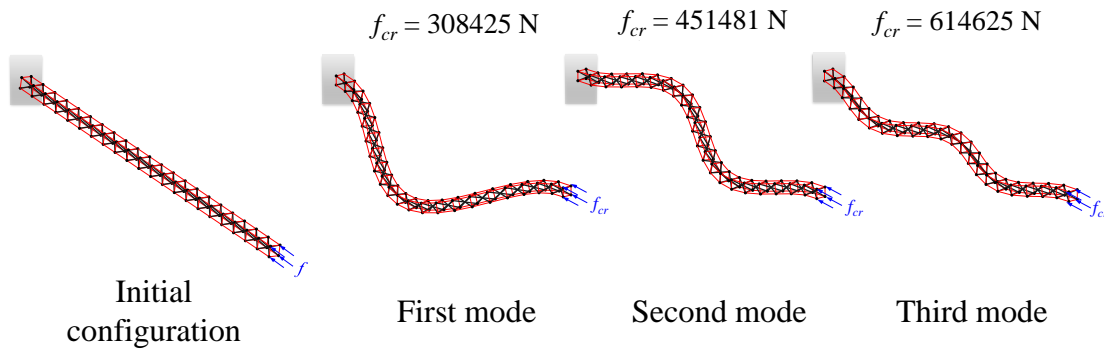


**Figure 2.** First three buckling modes of a tensegrity box structure with  $h = b = 0.05$  m,  $l = 1$  m, and  $q = 21$ . The box matches the first critical buckling force of a continuum beam with the same length and cross-section dimensions.

Figure 3(a) provides plots for  $\mu$  vs. complexity  $q$  for different values of beam cross-section dimensions  $b$  and  $h$  where the pre-stress in the tensegrity beam was optimized to minimize the mass and to match the first critical buckling load of the continuum beam. For this approach, the cross-section areas of the strings and bar members are calculated to avoid local failures in individual members (Goyal et al. 2020). The shaded region in Figure 3(a) is that where the mass of the tensegrity beam is lower than the mass of the continuum beam. The plot shows an increase in the mass ratio as the cross-section area of the beam increases. This can be understood as more pre-stress in a tensegrity is required to match the increased critical buckling force  $f_{cr}$  of a continuum beam with a larger cross-section area. Also, notice that the mass ratio increases with the complexity of the tensegrity structure, which is due to the fact that critical buckling force decreases with increased complexity (due to the increased flexibility of the structure) and hence more pre-stress is required to achieve the same critical buckling force as the continuum beam as complexity increases. The corresponding values of pre-stress parameter ( $\bar{\gamma}$ ) are shown in Figure 3(b).

Figure 4(a) shows the mass ratio of the tensegrity box structure with optimized areas of strings and bars to simultaneously match the first critical buckling force of the continuum beam and minimize the mass. The optimization of member cross-section areas gives less mass than only optimizing pre-stress values, which is observed by comparing the mass ratio from Figures 3 and 4. There are two types of strings in the structure: strings along the longitudinal directions and strings perpendicular to the longitudinal direction as shown in Figure 1. Figures 4(b) and 4(c) show the trend for the area of the strings along the longitudinal direction, denoted with area  $A_{s_1}$  and transverse direction, denoted by area  $A_{s_2}$ . The values of the cross-section area of the bars for all the combinations are shown in Figure 4(d).



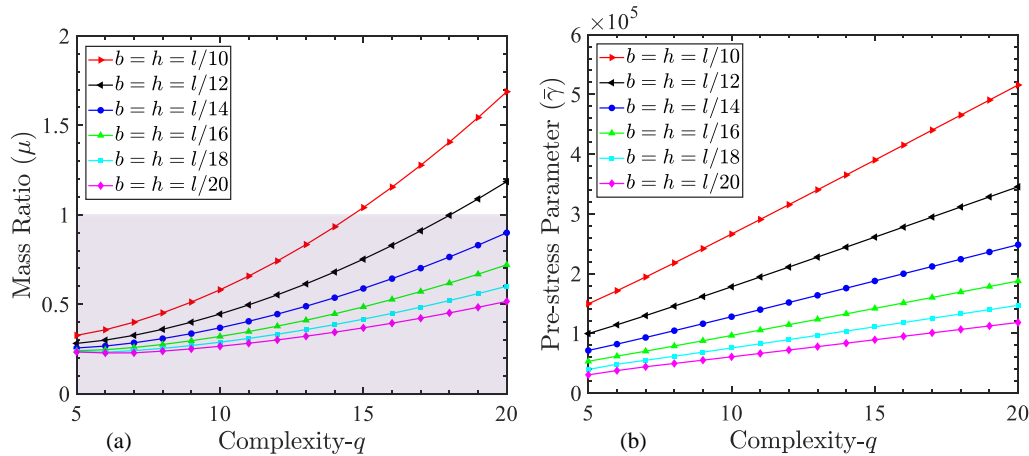


**Figure 3. (a) Mass ratio of tensegrity box vs. continuum beam for optimized *pre-stress* value. (b) The corresponding pre-stress parameter for different values of complexity.**

### Load free, pinned-pinned beam structure with target natural frequencies

Beam structures with pinned-pinned boundary conditions at their ends are considered in this example. The beams are not subjected to other boundary conditions such as applied external forces. Continuum solid beams and three-dimensional tensegrity box structures are considered for natural frequencies comparisons and mass assessments.

**Natural frequencies of a continuum solid beam.** The natural frequencies of pinned-pinned continuum solid beams are determined using Euler-Bernoulli beam theory. Again, the beam is composed of a linear elastic material with Young's modulus  $E_b$  and mass density  $\rho_b$ . The natural frequencies of the beam with a uniform rectangular cross-section with area  $A = bh$  and area moment of inertia  $I = bh^3/12$  are given as:

$$\omega = \left(\frac{i\pi}{l}\right)^2 \sqrt{\frac{E_b I}{\rho_b A}} = \left(\frac{i\pi}{l}\right)^2 \sqrt{\frac{E_b h^2}{12\rho_b}}, \quad i = 1, 2, 3, \dots, \quad (19)$$

where  $i$  represents the  $i^{\text{th}}$  natural frequency. The normalized deflections of the mode shape corresponding to the  $i^{\text{th}}$  natural frequency are given as:

$$\phi = \sin\left(\frac{i\pi x}{l}\right). \quad (20)$$

**Natural frequencies of a tensegrity box structure.** The tensegrity box structure shown in Figure 1 is also used to match the first three natural frequencies of the continuum beam counterpart with pinned-pinned boundary conditions.

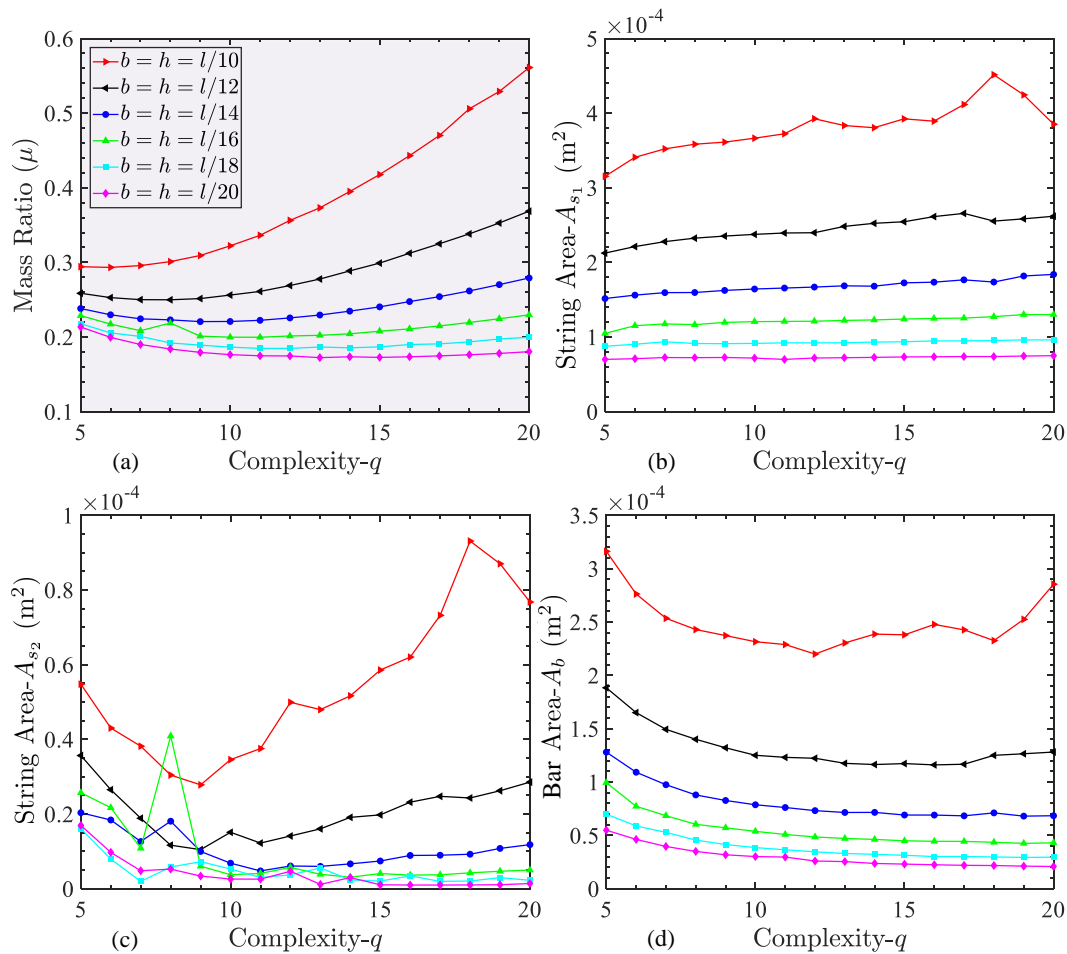


**Figure 4.** (a) Mass ratio of tensegrity box vs. continuum beam for optimized areas of strings and bars. (b, c, and d) Corresponding values for area of strings and bars for different values of complexity.

The goal is to match the unforced dynamic response of the continuum beam while minimizing the structural mass. For this task, the cross-section areas of the strings and bars are optimized (under a fixed pre-stress parameter  $\bar{\gamma}$ ) to match the first three natural frequencies of the continuum pinned-pinned beam. Figure 5 shows plots for mass ratio vs. complexity for different values of cross-sectional dimensions. Figure 5(a) shows the plots for a fixed pre-stress parameter value of  $\bar{\gamma} = 200$  while Figure 5(b) shows the same plot for  $\bar{\gamma} = 100$ . For both plots, the mass ratio  $\mu$  decreases with the increased dimensions of the cross-section. For all the curves, the mass ratio decreases monotonically with the increased complexity of the structure. As the complexity increases, the stiffness of the tensegrity structures decreases; hence, less mass is required to match the natural frequencies of the continuum beams (the natural frequencies of the tensegrity structures are proportional to their stiffness and inversely proportional to their mass).

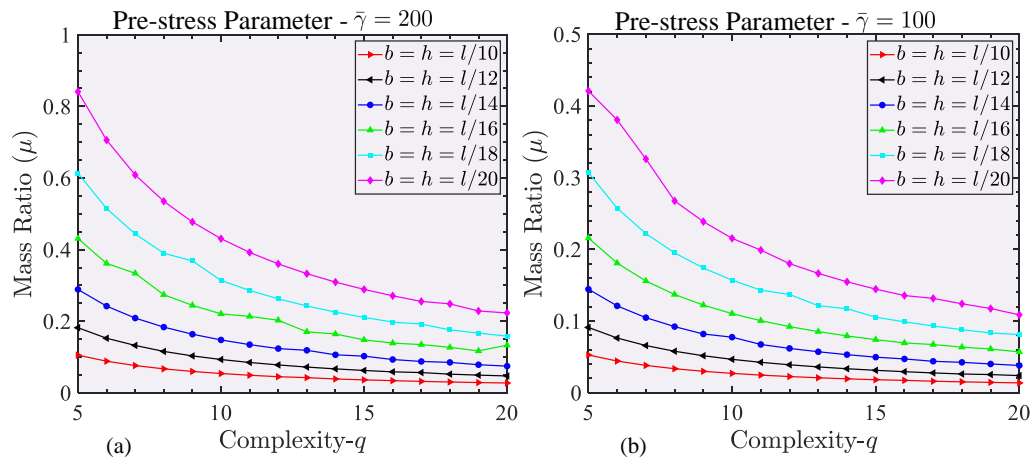


**Figure 5.** Mass ratio for 3D box structure with optimized areas of strings and bars to match the first three natural frequencies of a continuum pinned-pinned beam. (a) Fixed pre-stress parameter ( $\bar{\gamma} = 200$ ). (b) Fixed pre-stress parameter ( $\bar{\gamma} = 100$ ).

## CONCLUSIONS

This paper presented combined theoretical and computational approaches for the design of minimal mass tensegrity structures with modal requirements. Static modal requirements corresponding to critical buckling forces and dynamic modal requirements corresponding to natural frequencies were considered. The theory and computational approaches used to quantify both types of modes were derived through the linearization of the non-linear dynamics of tensegrity structures. These derivations were performed in a general fashion and thus the approaches are applicable to tensegrity structures of arbitrary shape and topology. Beam-like structures are considered for representative examples of the presented theoretical and computational approaches. The results from the examples show a large range of complexities and cross-section areas for which the mass required for tensegrity beams is lower than the mass required for continuum beams to match their first critical buckling force or their first three natural frequencies. The variables optimized to match the modal requirements included the pre-stress distribution and the cross-section areas of the bar and string members. Suggested future work in this topic includes designing more complex structures such as tensegrity domes and tensegrity habitats with targeted modal requirements.

## ACKNOWLEDGEMENT

This work was partially supported by the National Science Foundation under Award No. CMMI-1634590 and by Texas A&M University.

## References

- Carpentieri, G., Modano, M., Fabbrocino, F., Feo, L., and Fraternali, F. (2017). "On the minimal mass reinforcement of masonry structures with arbitrary shapes." *Meccanica*, 52(7), 1561–1576.
- Chan, W. L., Arbelaez, D., Bossens, F., and Skelton, R. E. (2004). "Active vibration control of a three-stage tensegrity structure." *Smart Structures and Materials 2004: Damping and Isolation*, Vol. 5386, International Society for Optics and Photonics, 340–346.
- De Tommasi, D., Maddalena, F., Puglisi, G., and Trentadue, F. (2017). "Fractality in selfsimilar minimal mass structures." *Journal of the Mechanics and Physics of Solids*, 107, 433–450.
- Goyal, R., Peraza Hernandez, E. A., and Skelton, R. (2019). "Analytical study of tensegrity lattices for mass-efficient mechanical energy absorption." *International Journal of Space Structures*, 34(1-2), 3–21.
- Goyal, R., Skelton, R., and Peraza Hernandez, E. A. (2020). "Design of minimal mass load-bearing tensegrity lattices." *Mechanics Research Communications*, 103, 103477.
- Goyal, R. and Skelton, R. E. (2019). "Tensegrity system dynamics with rigid bars and massive strings." *Multibody System Dynamics*, 46(3), 203–228.
- Johnston, B. G. (1983). "Column buckling theory: historic highlights." *Journal of Structural Engineering*, 109(9), 2086–2096.
- Ma, S., Yuan, X.-F., and Samy, A. (2019). "Shape optimization of a new tensegrity torus." *Mechanics Research Communications*, 100, 103396.
- MATLAB-fmincon (2020). "fmincon" <https://www.mathworks.com/help/optim/ug/fmincon.html>. Last accessed on 01/30/20.
- Nagase, K. and Skelton, R. (2014). "Minimal mass tensegrity structures." *Journal of The International Association for Shell and Spatial Structures*, 55(1), 37–48.
- Oppenheim, I. J. and Williams, W. O. (2001). "Vibration and damping in three-bar tensegrity structure." *Journal of Aerospace Engineering*, 14(3), 85–91.
- Peraza Hernandez, E. A., Goyal, R., and Skelton, R. E. (2018). "Tensegrity structures for mass-efficient planetary landers." *Proceedings of IASS Annual Symposia*, Vol. 27, International Association for Shell and Spatial Structures (IASS), 1–8.
- Rimoli, J. J. (2016). "On the impact tolerance of tensegrity-based planetary landers." *57th AIAA/ASCE/AHS/ASC Structures, Structural Dynamics, and Materials Conference*, 1511.
- Skelton, R. E. and de Oliveira, M. C. (2010). "Optimal complexity of deployable compressive structures." *Journal of the Franklin Institute*, 347(1), 228–256.
- van de Wijdeven, J. and de Jager, B. (2005). "Shape change of tensegrity structures: design and control." *Proceedings of the 2005, American Control Conference, 2005.*, IEEE, 2522–2527.
- Zhao, L. and Peraza Hernandez, E. A. (2019). "Theoretical study of tensegrity systems with tunable energy dissipation." *Extreme Mechanics Letters*, 32, 100567.